RESEARCH ARTICLE

Petrology of lavas from the 2004–2005 flank eruption of Mt. Etna, Italy: inferences on the dynamics of magma in the shallow plumbing system

Rosa Anna Corsaro · Lucia Civetta · Valeria Di Renzo · Lucia Miraglia

Abstract Following the 2001 and 2002–2003 flank eruptions, activity resumed at Mt. Etna on 7 September 2004 and lasted for about 6 months. This paper presents new petrographic, major and trace element, and Sr–Nd isotope data from sequential samples collected during the entire 2004–2005 eruption. The progressive change of lava composition allowed defining three phases that correspond to different processes controlling magma dynamics inside the central volcano conduits. The compositional variability of products erupted up to 24 September is well reproduced by a fractional crystallization model that involves magma already stored at shallow depth since the 2002–2003 eruption. The progressive mixing of this magma with a distinct new one rising within the central conduits is clearly revealed by the composition of the products erupted from 24 September to 15 October. After 15 October, the contribution from the new magma gradually becomes predominant, and the efficiency of the mixing process ensures the emission of homogeneous products up to the end of the eruption. Our results give insights into the complex conditions of magma storage and evolution in the shallow plumbing system of Mt. Etna during a flank eruption. Furthermore, they confirm that the 2004–2005 activity at Etna was triggered by regional movements of the eastern flank of the volcano. They caused the opening of a complex fracture zone extending ESE which drained a magma stored at shallow depth since the 2002–2003 eruption. This process favored the ascent of a different magma in the central conduits, which began to be erupted on 24 September without any significant change in eruptive style, deformation, and seismicity until the end of eruption.

Keywords Geochemistry · Isotopic compositions · Magma feeding system · Magma mixing · Mt. Etna

R. A. Corsaro (✉) · L. Miraglia
Sezione di Catania, Istituto Nazionale di Geofisica e Vulcanologia,
piazza Roma 2,
95123 Catania, Italy
e-mail: corsaro@ct.ingv.it

L. Civetta · V. Di Renzo
Sezione di Napoli, Istituto Nazionale di Geofisica e Vulcanologia,
via Diocleziano 328,
80124 Naples, Italy

L. Civetta · V. Di Renzo
Dipartimento di Scienze Fisiche, University of Napoli Federico II,
80124 Naples, Italy

Introduction

Recent flank eruptive activity of Mt. Etna is represented by three eruptions in 2001, 2002–2003, and 2004–2005. The first two have been widely studied from volcanological, geophysical, and petrologic points of view (see Allard et al. 2006 and references therein), and the research results showed a quite unusual eruption style among recent Mt. Etna activities. Flank eruptions, which occurred from 17 July to 9 August 2001 and from 26 October 2002 to 28 January 2003, were accompanied by significant seismicity and ground deformations; the eruptive vents were contemporaneously active on the south and north flanks of the volcano, resulting in strong explosions and lava flows of petrologically distinct two magmas. After 20 months of quiescence, activity resumed at Mt. Etna on 7 September 2004 and lasted for about 6 months. The absence of

significant geophysical anomalies preceding and accompanying the eruption onset (Di Grazia et al. 2006; Bonaccorso et al. 2006), the eruptive style exclusively effusive (Burton et al. 2005; Neri and Acocella 2006), and the variability of glass composition in the erupted lavas especially during the first weeks (Corsaro and Miraglia 2005) make the 2004–2005 eruption significantly different from the 2001 and 2002–2003 flank eruptions.

Here, we present a petrologic study performed on sequential samples collected throughout the 2004–2005 eruption. They provide an opportunity to identify complex processes operating in the volcano plumbing system, such as the fractional crystallization of an "eccentric" magma inherited from the 2002–2003 activity (Burton et al. 2005) and its progressive mixing with a distinct magma progressively rising along the central conduits. In the paper, "eccentric" is used according to Mt. Etna literature (Rittmann 1965; Tanguy 1980; Armienti et al. 1988). The eccentric eruptions are referred to as rare and generally highly explosive flank eruptions which are generated by dikes rising from depth bypassing the central volcano conduits. They emit sub-aphyric basaltic to trachybasaltic magma with mainly mafic phenocrysts. The most recent emission of this magma occurred during the 2001 and 2002–2003 flank eruptions from "Lower vents" and "Southern fissures" (Clocchiatti et al. 2004; Metrich et al. 2004; Andronico et al. 2005; Spilliaert et al. 2006; Viccaro et al. 2006; Corsaro et al. 2007), and the magma will hereafter be referred to as the 2001–2003 EC magma. However, the most commonly erupted magma at Mt. Etna during both flank and summit eruptions is different from this; that is, slightly evolved highly porphyritic trachybasalt with mainly plagioclase phenocrysts and derived from the central conduits system of the volcano. Recently, the latter type of magma was emitted from the "Upper vents" and "Northern fissures" during the 2001 and 2002–2003

eruptions and during the explosive activity of Mt. Etna summit craters (Bocca Nuova and Northeast craters), preceding the onset of the 2002–2003 flank eruption (June to September 2002). This is indicated as the 2001–2003 CC magma (Clocchiatti et al. 2004; Metrich et al. 2004; Andronico et al. 2005; Spilliaert et al. 2006; Viccaro et al. 2006; Corsaro et al. 2007). The existence of magmas rising along central conduits (CC-type magmas) and independently of them (EC-type magmas) has been documented since 1970s at Mt. Etna (see Corsaro and Pompilio 2004 and references therein) and their interaction is fundamental to explain compositional and isotopic variability of lavas emitted during the 2004–2005 eruption.

In this study we perform a detailed sampling of volcanics during the 2004–2005 eruption. The petrologic study allowed describing and modeling the conditions of magma storage and evolution inside Mt. Etna's plumbing system during the 2004–2005 activity, which occurred after two of the most important flank eruptions (2001 and 2002–2003) in recent times. Furthermore, we integrated the present petrologic data with previous geophysical investigations to understand a relationship among the dynamics of magmatic processes, eruption style, and flank instability of the volcano edifice during the 2004–2005 eruption.

Eruptive activity

The 2004–2005 Mt. Etna eruption occurred after 20 months of quiescence. Its onset was not heralded or accompanied by short-term precursory signals, such as seismicity and ground deformations, and neither by explosions at the summit craters (Burton et al. 2005). The event started on 7 September, when a complex fracture zone extended ESE (Fig. 1) from the Southeast Crater (SEC) toward the rim of Valle del Bove over a length of about 200 m. A small SE

Fig. 1 Map showing lava flow field during the 2004–2005 eruption with the index map in the *inset*. Positions and altitudes (m a.s.l.) of eruptive vents are shown. *SEC* Southeast Crater. Redrawn from "Reports of Istituto Nazionale di Geofisica e Vulcanologia, sezione di Catania", http://www.ct.ingv.it/Etna2004
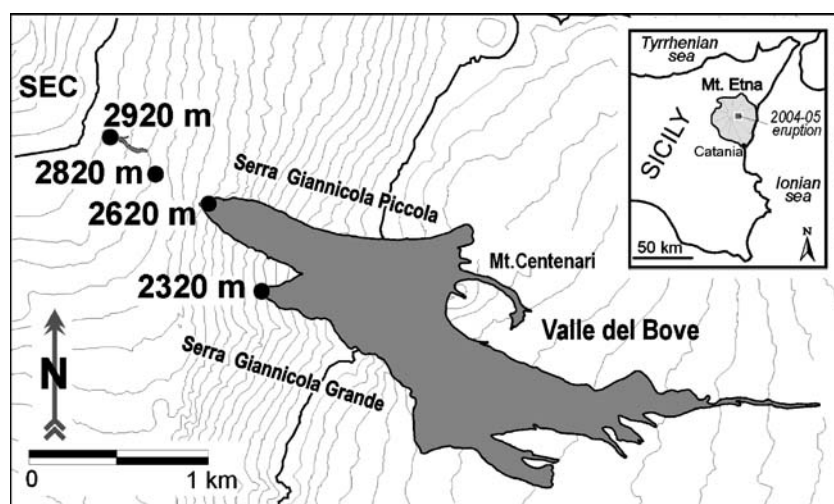
Table 1 Modal composition, chemistry of major and trace elements, and Sr–Nd isotopic ratios for the 2004–2005 lavas at Mt. Etna

Sample	070904A	070904C	070904G	100904B	110904B	130904A	130904C
Eruption date	07 Sept 2004	07 Sept 2004	07 Sept 2004	10 Sept 2004	11 Sept 2004	13 Sept 2004	13 Sept 2004
Fissure (m) a.s.l.	2,920	2,920	2,920	2,620	2,620	2,620	2,820
SiO_2	47.76	47.82	47.63	47.55	47.55	47.17	47.72
TiO_2	1.74	1.75	1.75	1.74	1.74	1.74	1.75
Al_2O_3	17.17	17.27	17.21	17.12	17.18	16.96	17.09
Fe_2O_3	1.74	1.76	1.76	1.74	1.74	1.70	1.76
FeO	8.71	8.79	8.77	8.69	8.72	8.51	8.78
MnO	0.18	0.18	0.18	0.18	0.18	0.18	0.18
MgO	5.19	5.25	5.18	5.20	5.20	5.18	5.32
CaO	10.62	10.60	10.54	10.56	10.58	10.39	10.73
Na_2O	3.56	3.56	3.58	3.56	3.59	3.54	3.53
K_2O	2.00	2.01	2.01	2.01	2.01	2.02	1.96
P_2O_5	0.58	0.58	0.59	0.58	0.58	0.57	0.58
L.O.I.	0.64	0.53	0.63	0.67	0.57	0.68	0.83
TOT	99.89	100.09	99.83	99.59	99.64	98.65	100.23
CaO/Al_2O_3	0.62	0.61	0.61	0.62	0.62	0.61	0.63
Mg#	0.47	0.47	0.47	0.48	0.47	0.48	0.48
Plagioclase	12.8			12.7			12.6
Clinopyroxene	7.7			4.3			4.3
Olivine	0.8			1.1			1.1
Ti-magnetite	0.2			0.6			0.5
P.I.	21.5			18.7			18.5
pl/mafic	1.5			2.1			2.1
Rb	50.1	51.7	53.3	52.1	53.8	54.9	53.1
Cs	0.9	1.0	1.0	1.0	1.0	1.0	1.0
Sr	1166	1199	1228	1204	1250	1267	1247
Ba	609	632	653	643	650	661	663
Ta	2.5	2.5	2.6	2.6	2.6	2.6	2.6
Th	7.2	7.5	7.7	7.7	7.7	7.6	7.7
U	2.1	2.2	2.3	2.3	2.2	2.3	2.2
Zr	206	207	215	211	218	222	220
Hf	4.5	4.6	4.8	4.7	4.8	4.8	4.8
Nb	40.8	41.6	42.9	41.7	43.3	44.3	43.5
La	55.1	56.7	58.5	57.8	58.4	59.4	59.1
Ce	107	110	114	113	114	116	116
Nd	47.4	48.9	50.8	50.2	50.7	51.0	51.0
Sm	9.1	9.5	9.8	9.7	9.8	9.9	9.9
Eu	2.8	2.9	3.0	3.0	3.0	3.0	3.0
Tb	1.05	1.07	1.12	1.10	1.10	1.11	1.12
Yb	2.23	2.27	2.36	2.32	2.33	2.35	2.36
Lu	0.3	0.3	0.4	0.3	0.4	0.4	0.3
Y	27.3	27.8	28.8	28.1	29.0	29.6	29.2
Ni	21	22	22	22	41	24	24
Cr	25.5	23.2	23.5	23.3	27.5	24.9	29.0
V	293	291	304	287	308	311	310
Co	37.0	38.0	39	37.2	39.4	40	39.8
Cu	123	127	133	132	137	139	132
$^{86}Sr/^{87}Sr$ WR	0.703632±8			0.703636±1			0.703644±9
$^{86}Sr/^{87}Sr$ Gl				0.703647±5			
$^{86}Sr/^{87}Sr$ Cpx				0.703621±8			
$^{86}Sr/^{87}Sr$ Ol							
$^{143}Nd/^{144}Nd$ WR				0.512854±9			0.512846±4
$^{143}Nd/^{144}Nd$ Gl				0.512839±5			
$^{143}Nd/^{144}Nd$ Ol							

The quoted error (2σ mean $N=180$) of the isotopes refers to the last digit

Mg# (Mg/(Mg+Fe^{2+}) moles), *plagioclase* sum (vol.%) of phenocrysts (1–3 mm) and microphenocrysts (0.5–1 mm), *P.I.* Porphyricity Index, *pl/mafic* plagioclase/(clinopyroxene + olivine + Ti-magnetite), *WR* whole rock, *Gl* glass, *Cpx* clinopyroxene, *Ol* Olivine

Table 1 (continued)

Sample	140904B	150904A	150904D	240904A	240904B	011004	041004
Eruption date	14 Sept 2004	15 Sept 2004	15 Sept 2004	24 Sept 2004	24 Sept 2004	01 Oct 2004	04 Oct 2004
Fissure (m) a.s.l.	2,320	2,620	2,320	2,320	2,620	2,620	2,620
SiO_2	47.94	47.69	47.50	47.88	47.78	47.47	47.37
TiO_2	1.76	1.76	1.75	1.78	1.77	1.76	1.76
Al_2O_3	17.33	17.17	16.89	17.27	17.23	17.09	17.14
Fe_2O_3	1.77	1.76	1.75	1.76	1.75	1.76	1.74
FeO	8.83	8.79	8.76	8.77	8.76	8.81	8.69
MnO	0.18	0.18	0.18	0.18	0.18	0.18	0.18
MgO	5.23	5.30	5.37	5.26	5.30	5.45	5.21
CaO	10.63	10.61	10.66	10.75	10.72	10.80	10.54
Na_2O	3.60	3.57	3.53	3.55	3.56	3.53	3.59
K_2O	2.04	2.02	1.98	2.07	2.06	2.02	2.05
P_2O_5	0.59	0.58	0.57	0.59	0.58	0.57	0.58
L.O.I.	0.59	0.52	0.63	0.77	0.79	0.70	0.78
TOT	100.48	99.95	99.59	100.62	100.50	100.14	99.62
CaO/Al_2O_3	0.61	0.62	0.63	0.62	0.62	0.63	0.61
Mg#	0.47	0.48	0.48	0.48	0.48	0.48	0.48
Plagioclase	12.0			13.5	11.7		11.0
Clinopyroxene	4.3			4.5	8.1		5.1
Olivine	0.9			1.4	2.2		1.5
Ti-magnetite	0.6			0.8	1.5		1.0
P.I.	17.8			20.2	23.4		18.7
pl/mafic	2.1			2.0	1.0		1.4
Rb	52.7	52.5	51.5	48.6	50.4	48.8	48.3
Cs	1.0	1.0	1.0	0.9	0.9	0.9	0.9
Sr	1221	1219	1185	1152	1175	1158	1156
Ba	647	653	632	599	618	631	618
Ta	2.5	2.5	2.5	2.3	2.4	2.4	2.4
Th	7.6	7.7	7.5	6.4	6.9	7.0	7.0
U	2.2	2.3	2.2	1.8	2.0	2.0	2.0
Zr	213	213	209	206	211	209	207
Hf	4.7	4.7	4.7	4.3	4.5	4.5	4.5
Nb	42.3	41.8	41.1	40.7	41.7	41.4	41.9
La	57.7	58.0	56.8	52.4	53.5	52.8	52.8
Ce	113	114	111	100	103	102	103
Nd	49.8	50.1	49.6	45.1	46.8	46.3	46
Sm	9.7	9.8	9.6	8.8	8.9	9.0	9.0
Eu	3.0	3.0	2.9	2.6	2.8	2.8	2.8
Tb	1.09	1.10	1.10	1.00	1.04	1.04	1.02
Yb	2.30	2.34	2.31	2.09	2.21	2.16	2.12
Lu	0.3	0.3	0.3	0.3	0.3	0.3	0.3
Y	28.3	28.2	28.0	27.1	27.3	27.2	26.9
Ni	22	22	24	24	25	26	24
Cr	22.6	23.9	28.8	26.6	29.9	35.8	28.1
V	298	294	299	306	315	322	308
Co	38.1	38.3	39	37.8	39.4	39.6	37.8
Cu	135	133	130	129	130	133	131
$^{86}Sr/^{87}Sr$ WR	0.703635±9			0.703637±7	0.703623±8		
$^{86}Sr/^{87}Sr$ Gl							
$^{86}Sr/^{87}Sr$ Cpx							
$^{86}Sr/^{87}Sr$ Ol							
$^{143}Nd/^{144}Nd$ WR	0.512845±8						
$^{143}Nd/^{144}Nd$ Gl							
$^{143}Nd/^{144}Nd$ Ol							

directed lava flow poured out at 2,920 m a.s.l. and stopped a few hours later. On 9 September, a portion of the fracture zone collapsed at 2,820 m a.s.l and a pit was formed, emitting dense white vapors and occasional bombs and lapilli on 13 September. A new effusive vent opened at 2,620 m a.s.l. on 10 September and fed a lava flow expanding towards the Serra Giannicola Piccola ridge. Then, the fracture zone propagated downslope and a new effusive vent opened at about 2,320 m a.s.l. close to Serra Giannicola Grande. After 13 September, the fracture zone

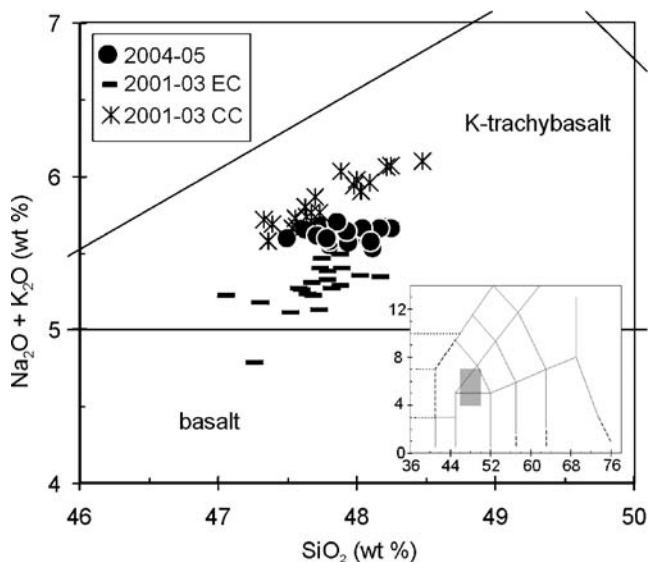| 071004	161004	231004	011104	231104	140105	300105	250205A
07 Oct 2004	16 Oct 2004	23 Oct 2004	01 Nov 2004	23 Nov 2004	14 Jan 2005	30 Jan 2005	25 Feb 2005
2,320	2,620	2,620	2,620	2,620	2,620	2,620	2,620
47.59	47.76	47.68	47.35	47.55	47.42	47.49	47.81
1.76	1.74	1.74	1.75	1.75	1.72	1.74	1.73
17.06	17.12	16.97	16.95	17.10	16.90	16.88	16.75
1.77	1.74	1.74	1.73	1.75	1.74	1.74	1.77
8.83	8.68	8.70	8.66	8.76	8.67	8.70	8.84
0.18	0.18	0.18	0.18	0.18	0.18	0.18	0.19
5.50	5.35	5.41	5.40	5.46	5.52	5.53	5.83
10.83	10.82	10.78	10.62	10.64	10.74	10.78	10.93
3.54	3.64	3.62	3.62	3.65	3.59	3.56	3.57
1.99	2.00	2.00	1.99	2.03	1.99	2.00	1.97
0.57	0.57	0.58	0.56	0.58	0.57	0.57	0.56
0.72	0.59	0.53	0.59	0.63	0.62	0.61	0.59
100.34	100.18	99.92	99.40	100.09	99.66	99.79	100.53
0.64	0.63	0.64	0.63	0.62	0.64	0.64	0.65
0.48	0.48	0.48	0.49	0.48	0.49	0.49	0.50
12.8		12.3		10.2	11.3		10.5
4.7		5.9		4.9	5.7		10.5
1.4		1.8		2.0	2.6		1.9
0.5		0.8		0.3	0.1		0.2
19.4		20.9		17.3	19.6		23.1
1.9		1.4		1.4	1.4		0.8
48.4	47.4	46.5	48.5	48.4	47.9	47.0	46.9
0.9	0.9	0.9	0.9	0.9	0.9	0.9	0.9
1164	1162	1149	1173	1166	1148	1134	1145
624	637	634	640	647	628	618	625
2.5	2.6	2.5	2.6	2.6	2.5	2.5	2.6
7.1	7.3	7.3	7.5	7.4	7.2	7.1	7.3
2.0	2.1	2.1	2.2	2.1	2.1	2.0	2.1
210	211	211	215	214	211	207	211
4.6	4.6	4.5	4.6	4.6	4.5	4.5	4.6
42.2	43.5	43.6	44.2	44.9	43.1	42.8	43.6
52.8	53.1	52.9	53.3	54.2	52.3	51.6	52.3
104	106	105	111	112	104	108	110
47	48	48	49	49	48	48	48
9.2	9.3	9.0	9.5	9.3	9.3	9.2	9.4
2.8	2.8	2.8	2.9	2.8	2.8	2.8	2.9
1.04	1.05	1.04	1.06	1.05	1.04	1.03	1.05
2.19	2.20	2.16	2.24	2.20	2.23	2.20	2.23
0.3	0.3	0.3	0.3	0.3	0.3	0.3	0.3
27.2	27.3	27.4	27.9	27.8	27.4	27.1	27.6
27	26	26	27	28	28	28	31
39.2	36.7	35.3	37.4	37.1	39.6	45.1	45.1
320	313	315	322	317	317	316	329
39.8	38.3	38.4	39.4	40.0	39.5	38.4	40.7
133	132	132	131	134	135	128	137
0.703603±9		0.703588±9		0.703577±9	0.703596±6		0.703597±8
							0.703590±6
							0.703578±6
							0.703596±6
0.512864±10		0.512872±12					0.512871±5
							0.512854±4
							0.512850±5

The quoted error (2σ mean $N=180$) of the isotopes refers to the last digit

did not evolve further, and the effusive activity was stabilized at both 2,620 and 2,320 m vents. During the next months, a compound lava field developed and reached about 1,600 m a.s.l. The lava field was characte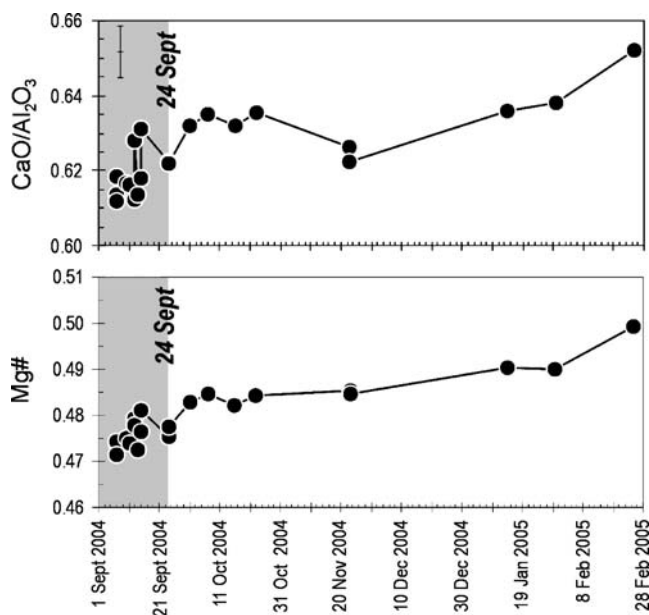rized by complex lava tubes in the upper portion and several ephemeral vents in the central portion. On 8 March, the eruption finished. The total volume of lava flows was estimated at 40,000,000 m³ by Neri and Acocella (2006) and 60,000,000 m³ by D. Andronico (2006 pers. comm.).

Sampling and analytical methods

We collected samples from lava flows near the vents. Sampling was not a simple task since the emission points were located on the steep and rugged western flank of the Valle del Bove. It was snowy from December to the end of the eruption, accounting for the scarcity of samples in that period. Modal analyses are based on 1,500 counts/sample. All the estimated values are in volume percent and are recalculated on a vesicle-free basis. Mineral chemistry are measured at Istituto Nazionale di Geofisica e Vulcanologia, sezione di Catania with a LEO-1430 scanning electron microscope (SEM), equipped with an Oxford EDS micro-analytical system. Analytical conditions are 20 keV of acceleration tension, 1.2 nA of beam current and XPP data reduction routine. Replicate analyses of the mineral standards (Chromium augite NMNH 164905, Olivine San Carlos USNM 11131/444, Plagioclase Labradorite USNM115900, Horneblende Kakanui USNM143965, apatite Durango USNM104021, Chromite USNM117075, see Jarosewich et al., 1980) ensure an analytical precision, expressed as relative standard deviation, less than 1% for SiO_2, Al_2O_3 and FeO; 0.5% for MgO and CaO; between 2 and 3% for TiO_2, Na_2O and K_2O (Miraglia, 2006). Major and trace elements of bulk rock have been measured at the Centre National de la Recherche Scientifique, Centre de Recherches Pétrographiques et Géochimiques (CNRS-CRPG), Vandoeuvre Les Nancy Cedex, France, respectively, by inductively coupled plasma atomic emission spectroscopy (for SiO_2, TiO_2, Al_2O_3, FeOtot, MgO. MnO, CaO, Na_2O, K_2O, and P_2O_5) and

Fig. 3 Temporal variations of CaO/Al_2O_3 and $Mg\#=Mg/(Mg+Fe^{2+})$ moles, for the 2004–2005 lavas. The most evolved products are erupted before 24 September. Analytical uncertainty is 1σ

inductively coupled plasma mass spectrometry (for Rb, Cs, Sr, Ba, Ta, Th, U, Zr, Hf, Nb, La, Ce, Nd, Sm, Eu, Tb, Yb, Lu, Y, Ni, Cr, V, Co, Cu; Carignan et al. 2001). Analytical uncertainty (1σ) is: <1% for SiO_2 and Al_2O_3, <2% for Fe_2O_3, MgO, CaO, Na_2O, K_2O, <5% for MnO, and TiO_2 and 5–10% for P_2O_5, and <5% for all trace elements except U (<8%). Sr and Nd isotope analyses have been performed by Thermal Ionization Mass Spectrometer Triton TI at the Istituto Nazionale di Geofisica e Vulcanologia, sezione di Napoli. The Sr and Nd contents in blanks were small enough for the analyzed samples during the measurement period. The mean measured value of $^{87}Sr/^{86}Sr$ for the standard NIST-SRM987 was 0.710250 ± 0.000014 (2σ, $N=56$) and that of $^{143}Nd/^{144}Nd$ for the La Jolla standard was 0.511843 ± 0.000015 (2σ, $N=25$). Details on the techniques used are in Di Renzo et al. (2007). Modal mineralogy, whole rock major oxides, trace elements and Sr–Nd isotope analyses of 2004–2005 lavas are reported in Table 1. The compositions of the 2004–2005 lavas are compared with those of products emitted during the 2001 and 2002–2003 eruptions (Corsaro et al. 2007; Electronic supplementary material; L. Civetta, 2004 unpublished, for Sr and Nd isotopic ratios of the 2001 eruption).

Petrography

Plagioclase, clinopyroxene, olivine, and Ti-magnetite form the mineralogical assemblage of 2004–2005 lavas. The nature, abundance, relative proportions, and mineral chemistry of phenocrysts are similar, showing limited ranges

Fig. 2 Lavas erupted during the 2004–2005 eruption in total alkali vs. silica diagram of Le Maitre et al. 2002. The *gray-colored area in the inset* comprises the studied lavas. Analytical uncertainty is 1σ. The composition of the 2001–2003 CC and EC lavas is also plotted for comparison (Corsaro et al. 2007; Electronic supplementary material)

throughout the eruption with the exception of the sample erupted on 25 February, which is distinct for the higher clinopyroxene abundance (Table 1). All the analyzed samples show porphyritic texture. Porphyricity Index (total abundance of mineral phases) varies between 17.3 and 23.4 vol.%, and pl/mafic (plagioclase/(clinopyroxene + olivine + Ti-magnetite)) ranges from 0.8 to 2.1 (Table 1).

Plagioclase phenocrysts range between 1 and 3 mm in size, vary from 5.2 to 8.9 vol.%, and are mostly euhedral with sieve texture at the core or concentric zoning in the rim. Sieved and clear plagioclase frequently coexist in the same sample. Anhedral crystals are common among large plagioclase phenocrysts. Microphenocrysts of plagioclase ranging from 0.5 to 1 mm in size are from 4.5 to 6.8 vol.%, and are mostly euhedral. Phenocrysts and microphenocrysts with normal zoning (An_{84} to An_{63}) and oscillatory zoning (An_{82} core, An_{85} intermediate zone, An_{65} rim) coexist in the same sample. The composition of groundmass microlites (<100 μm) ranges An_{70-50}. The average composition of microlites is An_{57} and remains nearly constant throughout the eruption, with the exception of a lava erupted on 1 October 2004 (sample 011004) where more calcic microlites (average An_{62}) were found.

Phenocrysts of clinopyroxene (4.3–10.5 vol.%) ranging from 1 to 5 mm across, are euhedral and frequently enclose opaque minerals. The large crystals mostly show a zoning with the sectors of different Mg# ($Mg/(Mg + Fe^{2+})$), whose average values are 0.73 and 0.78, respectively. Crystals with sector and oscillatory zoning are often observed in the same sample.

Olivine phenocrysts (0.8–2.6 vol.%) range from 0.5 to 1 mm across. The large crystals are frequently resorbed, while the smallest ones are generally subrounded in shape. Olivine generally shows normal zoning from the core (Fo_{80}) to the rim (Fo_{75}), with the exception of large crystals with oscillatory zoning (Fo_{73} core, Fo_{76} intermediate zone, Fo_{70} rim). Groundmass olivine microlites (<100 μm) vary in composition from Fo_{75} to Fo_{68}. Scarce (0.1–1.5 vol.%) Ti-magnetite phenocrysts, ranging from 36 to 40 in Usp, are also present.

Glomeroporphyritic clusters of mafic minerals are common in all samples. They are generally from 1 to 5 mm in diameter and are formed of 3–10 crystals of clinopyroxene, opaque oxides, and olivine in order of abundance and frequent embedded glass. Plagioclase is practically absent. The groundmass texture varies from glassy to hyalopilitic, consisting of brown glass, embedding plagioclase, and mafic minerals.

Geochemistry of bulk rock

Products of the 2004–2005 eruption are K-trachybasalts (Le Maitre 2002) with average SiO_2%=47.92 (±0.19, 1σ) and

alkalies %=5.62 (±0.05, 1σ). They are intermediate in composition (Fig. 2) between 2001 and 2003 both the EC and CC magmas (Corsaro et al. 2007; Electronic supplementary material).

Throughout the eruption, major elements variability is rather limited. Temporal variation of compositional parameters such as CaO/Al_2O_3 and Mg# (Fig. 3) show that the most evolved products are erupted before 24 September, and then the ratios increase slightly. The highest values
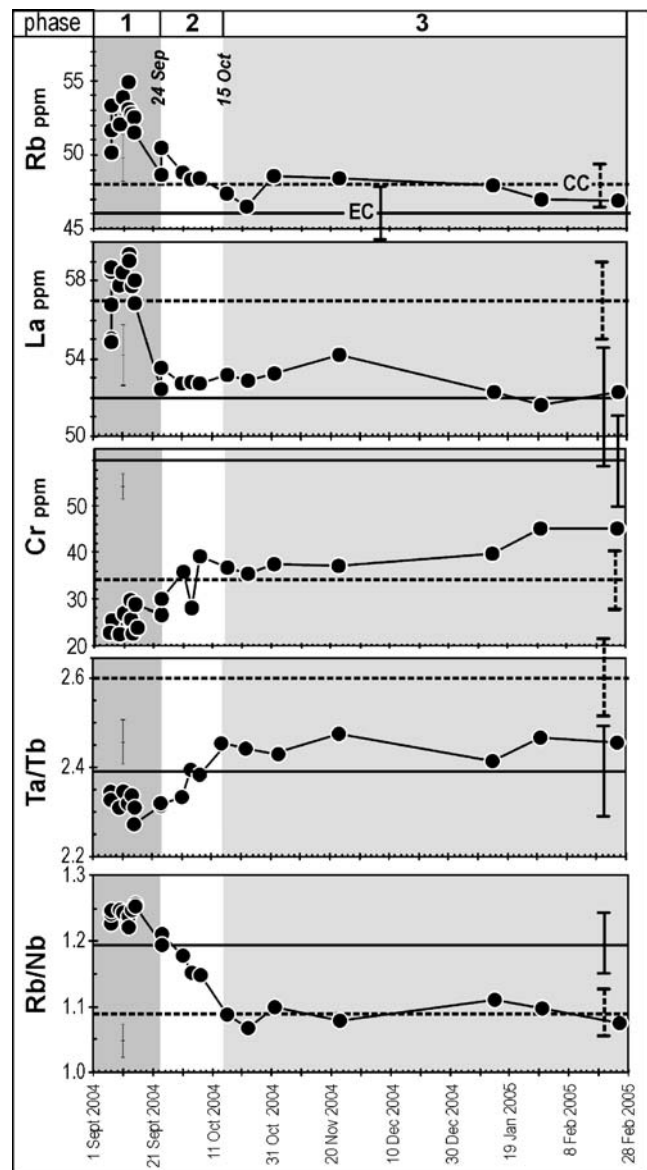
Fig. 4 Temporal variations of Rb, La, Cr, Ta/Tb, and Rb/Nb for the 2004–2005 lavas; Three distinct trends and corresponding three phases are evident: pre-24 September (*phase 1*), 24 September to 15 October (*phase 2*), and post-15 October (*phase 3*). Analytical uncertainty is 1σ. *Continuous line* average value and standard deviation (±σ) of the 2001–2003 EC lavas. *Dashed line* average value and standard deviation (±σ) of the 2001–2003 CC lavas (Corsaro et al. 2007; Electronic supplementary material)

Fig. 5 Sr and Nd isotopic ratios for bulk rock, matrix glass, and olivine for the 2004–2005 lavas. For the meaning of phases, see Fig. 4. *BR* bulk rocks, *GL* matrix glass, *OL* olivine. In the *inset*, the 2004–2005 lavas are compared with the Sr–Nd isotopic fields of subalkaline, prehistoric alkaline, pre-1974 AD historic, and post-1974 AD products (e.g., Corsaro and Pompilio, 2004)
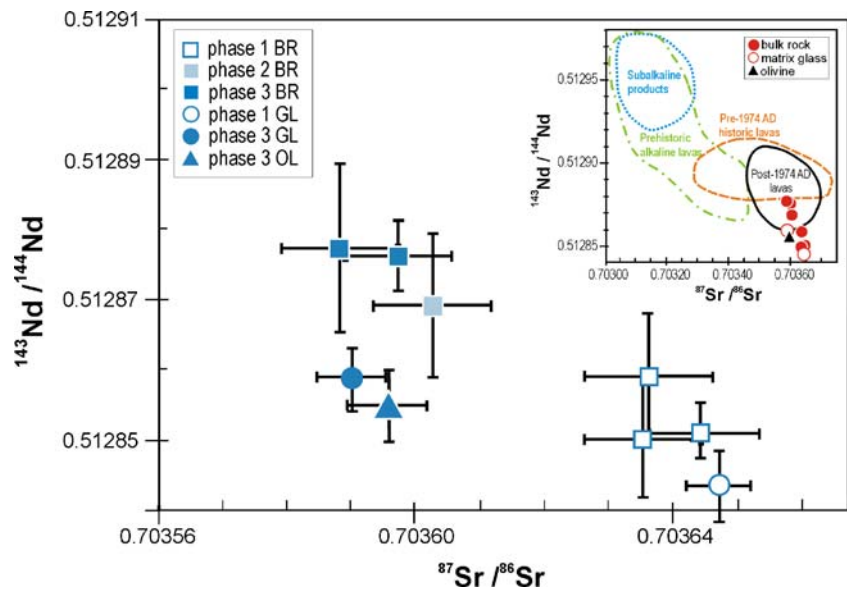

($CaO/Al_2O_3=0.65$ and Mg#=0.50), measured in products erupted on 25 February, are most likely due to the higher content of mafic phenocrysts as shown in modal analysis.

Temporal variations of trace elements (Fig. 4) reveal that most evolved magmas are erupted before 24 September, and the lavas before 24 September show higher content of incompatible elements and lower contents of compatible elements. After 24 September, incompatible elements (e.g., Rb, La) of the lavas decrease, whereas compatible elements (e.g., Cr) increase. From 15 October up to the end of the eruption, most trace elements do not show significant variations. The lavas erupted until 24 September are more enriched in incompatible elements and depleted in compatible elements than 2001–2003 CC and EC lavas (Corsaro et al. 2007; data in Electronic supplementary material; Fig. 4). After 24 September, the trace elements content overlaps between CC and EC products. The ratios of incompatible elements (Fig. 4), which hardly change through fractional crystallization (e.g., Ta/Tb) and are modified by contribution of aqueous fluids (e.g., Rb/Nb), clearly divide the 2004–2005 eruption into three phases: pre-24 September lavas (hereafter phase 1), characterized by the highest Rb/Nb and lowest Ta/Tb, lavas from 24 September to 15 October (phase 2) showing a decrease in Rb/Nb and increase in Ta/Tb, and post-15 October lavas (phase 3) with constant ratios in both Rb/Nb and Ta/Tb.

Sr and Nd isotopic ratios

Sr and Nd isotopic ratios of the 2004–2005 lavas range from 0.70358 to 0.70364 and from 0.512870 to 0.512845, respectively. The Sr and Nd isotopic ratios are negatively
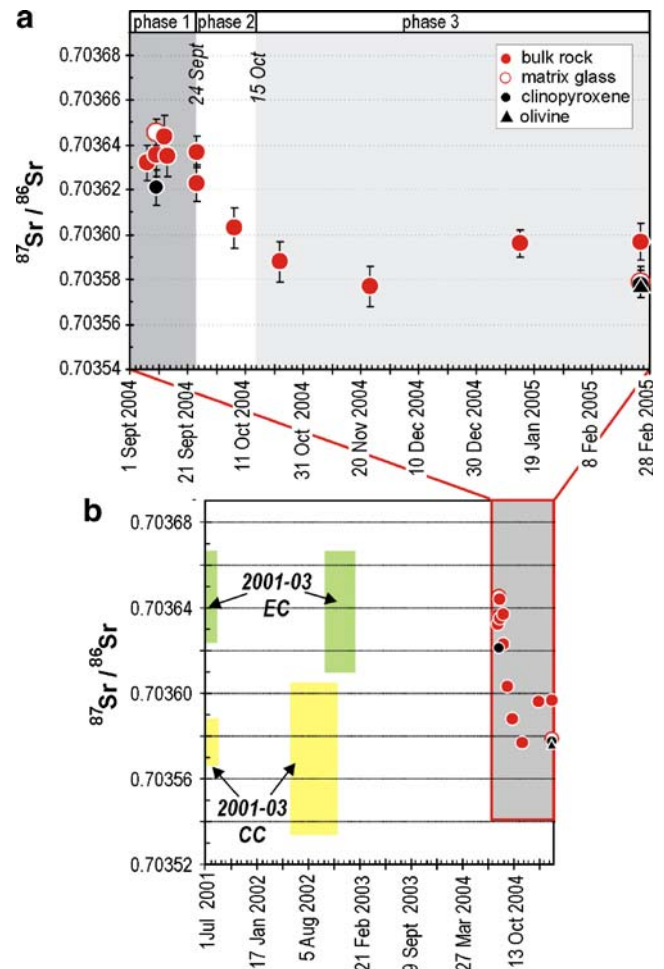
Fig. 6 a Temporal variation of the Sr isotopic ratios of bulk rocks, matrix glass, clinopyroxene, and olivine for the 2004–2005 lavas. **b** Comparison with products of the 2001–2003 CC and EC eruptions (L. Civetta, 2004 unpublished; Electronic supplementary material)
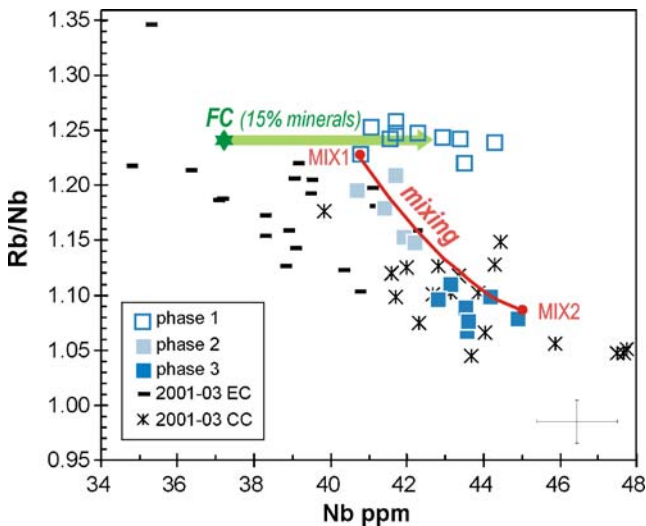
Fig. 7 Rb/Nb vs. Nb for the 2004–2005 lavas, 2001–2003 CC and EC products (Corsaro et al. 2007; Electronic supplementary material). *FC* modeled fractional crystallization trend starting from the average composition of selected 2002–2003 EC lavas (*star*). See the text for details. Binary mixing has been modeled between *MIX1* (the most primitive composition of the phase 1 lavas) and *MIX2* (the average composition of the 2002–03 CC magmas). See the text for details. Analytical uncertainty is 1σ

correlated and are plotted within the Etna Sr–Nd isotopic array, mostly in the field of post-1974 volcanics (Fig. 5).

Three phases are confirmed by the temporal variation of Sr and Nd isotopic ratios (Figs. 5 and 6a). In phase 1, rocks are the most enriched in radiogenic Sr and the least enriched in radiogenic Nd of the 2004–2005 lavas. Groundmass and clinopyroxene are in equilibrium isotopically. In phase 2, the Sr isotopic ratio decreases down to 0.70358, while the Nd isotope ratio increases up to 0.512870. The Sr and Nd isotopic ratios remain constant in phase 3. Groundmass and olivine, separated from one sample at the end of the eruption, are in equilibrium isotopically (Fig. 6a).

This result clearly indicates the involvement of at least two isotopically distinct magmatic components during the eruption; one has $^{87}Sr/^{86}Sr$ of 0.70364 and $^{143}Nd/^{114}Nd$ of 0.512845, and the other is less radiogenic, with $^{87}Sr/^{86}Sr$ of 0.70358 and $^{143}Nd/^{114}Nd$ of 0.512870. The most radiogenic component is found in phase 1, whereas the least radiogenic one is in phase 3. Lavas of phase 2 are intermediate between phases 1 and 3. The least radiogenic lavas in phase 3 are isotopically similar to the 2001–2003 CC products (Fig. 6b), whereas the most radiogenic ones in phase 1 are akin to the 2001–2003 EC magmas.

Discussion

Geochemical and isotopic data of magmas erupted over the 2004–2005 eruption clearly display temporal compositional

variations. Products of phase 1 (pre-24 September) are the most evolved and radiogenic of the 2004–2005 eruption. They are akin to the 2001–2003 EC lavas, whereas lavas of phase 3 (post-15 October) show the affinity with the 2001–
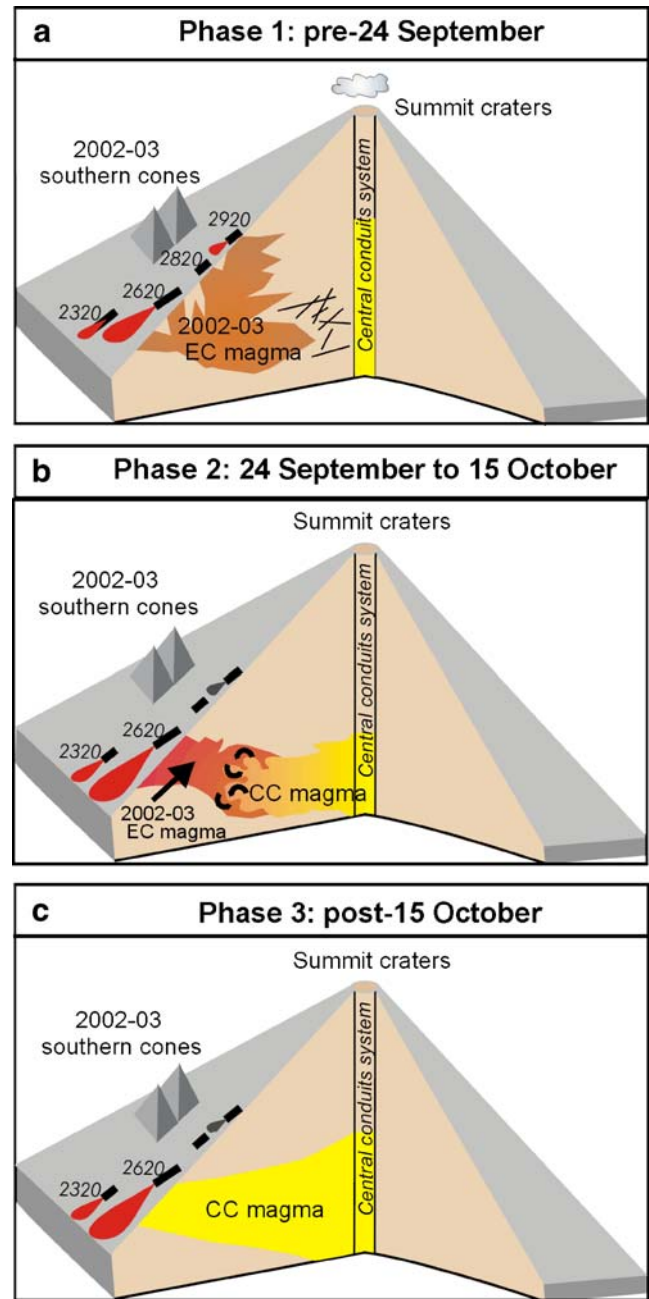
Fig. 8 Cartoon illustrating the shallow plumbing system of Mt. Etna during the 2004–2005 eruption. a *phase 1*: the erupted magma had been stored in a small reservoir since the "eccentric" 2002–2003 eruption and have evolved through the closed-system fractional crystallization. b *phase 2*: the remaining phase 1 magma was mixed progressively with a magma coming from the central conduits. c *phase 3*: the eruption fed by the magma rising in the central conduits had continued till the end of the 2004–2005 eruption
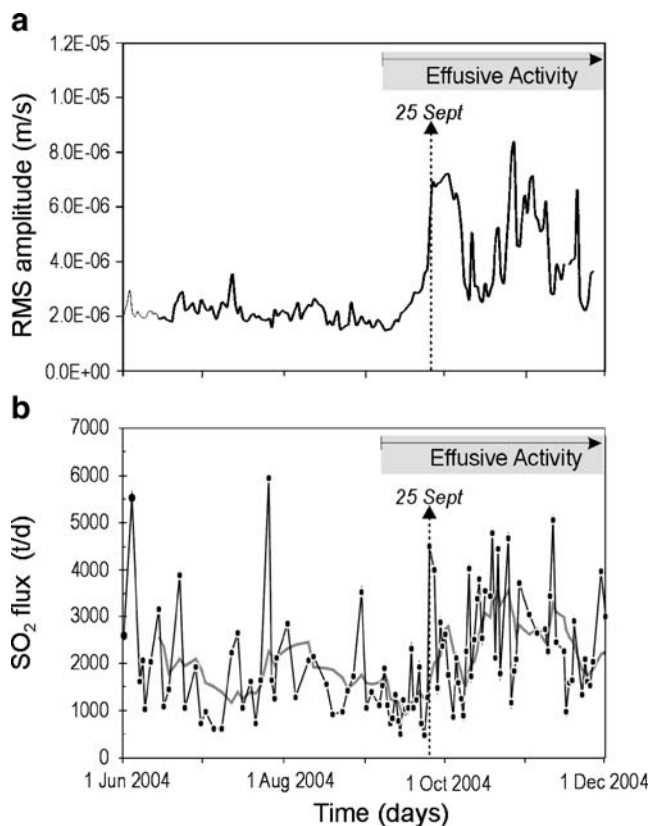
Fig. 9 Temporal variations of the root mean square amplitude of volcanic tremors (*RMS*) (**a**) and SO₂ flux with COSPEC (**b**) for the period covering 3 months before and after the 2004 eruption. RMS represents 25th percentile values of the daily average which was modified from Di Grazia et al. (2006). The amplitude was calculated over 30 s time windows at the station ECPN. The SO₂ flux (*black line*) was modified from Burton et al. (2005). *Thick gray curve* represents a 7-day moving average. Both variations show a sharp increase on 25 September

2003 CC volcanics. Lavas of phase 2 (from 24 September to 15 October) are intermediate between phases 1 and 3.

We first considered whether the chemical variations of 2004–2005 lavas could be due to a crystal-liquid fractionation (FC) process or not. However, this model was ruled out since the Sr and Nd isotopic ratios are variable beyond the analytical uncertainty. Alternatively, we propose another model, where the compositional variation in the 2004–2005 lavas reflects three distinct phases in the shallow plumbing system of Mt. Etna.

Phase 1 (pre-24 September)

The products of phase 1 are the most evolved of the eruption (Figs. 3 and 4), and their Sr and Nd isotopic ratios are similar to the 2001–03 EC products (Fig. 5b). We suggest that this similarity reflects the presence of a small reservoir, where magma had remained since the last

"eccentric" 2002–2003 eruption (Burton et al. 2005), and its composition was modified with time by closed-system fractional crystallization until the 2004–2005 eruption. Several lines of evidence support this hypothesis.

In a plot of Nb vs. Rb/Nb (Fig. 7), phase 1 lavas define a horizontal trend, which is consistent with a FC process that poorly affects incompatible elements ratios. To model the FC process, we performed mass balance calculations, assuming the average composition of 2002–2003 EC samples (281002A, 041102A, 191102, 291102, selected because their Sr isotopic ratios are similar to phase 1 rocks, see analyses in Electronic supplementary material) as parental magma and the average of 2004–2005 lavas erupted before 24 September (Table 1) as the daughter magma. Based on the petrographic evidence, plagioclase (An=70), olivine (Fo=74), clinopyroxene (Mg#0.76), and Ti-magnetite (Usp=32) were used as fractionating mineral phases. The sum of the residuals in this mass balance calculation was $r^2=0.14$, after the removal of 15% crystals (7% plagioclase, 3% olivine, 4% clinopyroxene, and 1% Ti-magnetite). Mass balance has been tested also using trace elements with the Rayleigh's equation and partition coefficients from D'Orazio et al. (1998). The results confirm the effectiveness of the proposed FC process, since discrepancies between modeled and real values are less than 5% for most trace elements. In particular, the modeled FC trend from the 2002–2003 EC parental magma to the average 2004–2005 daughter magma is plotted in Fig. 7, where it matches well the real distribution of samples erupted before 24 September.

Thus, a qualitative approach and quantitative treatment of data lead us to propose the following scenario to explain magma dynamics before 24 September. The eruption started with the opening of a fracture zone extending ESE that tapped and flushed a batch of magma stored at very shallow level since the 2002–2003 EC activity. The position of the uppermost eruptive vents at 2,920 m a.s.l. suggests that the top of the reservoir was probably located at about 300–400 m below the summit craters (Fig. 8a). The magma stored in this reservoir since the 2002–2003 EC eruption degassed and evolved through closed-system fractional crystallization, because no refilling of new magma was detected by the petrological data. This "quiet" circumstance may explain the lack of precursory geophysical signals (earthquake swarms, increases in tremor amplitude, and rapid ground deformations) before the onset of the 2004–2005 eruption, contrasting to the case of 2001 and 2002–2003 flank eruption in which a new magma progressively rose from depth. This supports the hypothesis that the 2004–2005 eruption was triggered by the movement of the east flank of the volcano, as suggested from structural and geodetical data by Burton et al. (2005), Neri and Acocella (2006), and Bonaccorso et al. (2006). It is

noteworthy that the trend of the 2004–2005 eruptive fractures matched well the ESE-WSW tensile stress indicated by ground deformation from 2003 to 2004 (Bonaccorso et al. 2006). The minimum size of this magma batch at the time of 2004–2005 eruption must correspond to the volume of magma erupted before 24 September. Assuming an effusion rate of 2–4 m³/s (see "Reports of Istituto Nazionale di Geofisica e Vulcanologia, sezione di Catania", http://www.ct.ingv.it/Etna2004) and a bulk vesicularity of 20 vol.%, the volume of magma was between 2,300,000 and 4,600,000 m³ as dense rock equivalent. The volume corresponds to a hypothetical spheroid magma pocket with the minimum height of 600 m (the difference between the uppermost and lowermost vents active before 24 September) and the diameter of 270 to 390 m, for a volume, respectively, of 2,300,000 or 4,600,000 m³. The magma batch of this dimension is similar to a shallow conduit and/or a network of dikes where compositional and thermal zoning of magma develop inside. The zoning is suggested by eruption of variously evolved lavas in phase 1 (see their horizontal spreading in Fig. 7) and has already been pointed out by Corsaro and Miraglia (2005) based on a strong variability of the matrix glass chemistry and of the eruptive temperatures before 24 September.

Phase 2 (24 September to 15 October)

The composition of lavas in phase 2 progressively changed with time and shifted towards CC magma (Figs. 4, 5, and 6). The different geochemical features of phase 2 from phases 1 and 3 are also evident in Fig. 7, where phase 2 lavas significantly depart from the FC horizontal trend and point towards the 2001–2003 CC magma. This pattern precludes derivation of phase 2 magma from phase 1 magma through FC process and suggests its origin from a mixing between the phase 1 magma and a new magma, probably arriving from the central conduits.

We tested a binary mixing model according to Langmuir et al. (1978). We chose the most primitive composition of phase 1 lavas (sample 070904A; MIX1 in Fig. 7, Nb=40.8, Rb=50.1) and the average composition of the 2002–2003 CC lavas (MIX2 in Fig. 7, Nb=45.0, Rb 48.9; 2002-03 CC lavas in Electronic supplementary material) as end members. Model calculations show that the compositional variation of phase 2 lavas can be explained by progressive mixing from 10% to 50% of the 2002–2003 CC magma with phase 1 magma. Mixing of different magmas is supported by petrographic lines of evidence such as oscillatory zoning in plagioclase and clinopyroxene and disequilibrium textures (e.g., sieved or dusty plagioclase). The coexistence of resorbed and euhedral plagioclase and olivine in the same sample, and of normally zoned plagioclase and reversely zoned plagioclase, may further strengthen the hypothesis of mixing. Groundmass plagioclase microlites which crystallized at shallow depth (Metrich and Rutherford 1998) show a significant increase in anorthite content (An_{62}) in a sample erupted on 1 October, probably recording the arrival of slightly more primitive CC-type magma.

Thus, the petrological data suggest that in phase 2 the EC magma became mixed with the CC magma, the latter of which had remained in a shallow part of the plumbing system during phase 1. It is expected that this mixing was induced by propagation of the ESE fracture zone inwards (Fig. 8a). Decreasing magma pressure in the reservoir of phase 1 magma, due to loss of magma by eruption, may have permitted successive intrusion of the CC magma from the central conduits (Fig. 8). The fact that the magma plumbing system was changed by the depressurization after 24 September may be verified by geophysical and geochemical observations such as a remarkable increase in the amplitude of tremor on 25 September (Di Grazia et al. 2006) and SO_2 flux peaked since 25 September (Burton et al. 2005; Fig. 9). The chemical variation of the phase 2 lavas is characterized by a rapid decrease of EC magma in the mixing and a progressive shifting towards CC magma composition. This is a good indication that the mixing is a syn-eruptive process which occurred quickly and operated efficiently essentially in phase 2.

Phase 3 (post-15 October)

After 15 October till the end of the eruption, the contents of most incompatible elements and the Sr–Nd isotopic ratios (Figs. 4, 5, and 6) remain fairly constant and are very close to the values of the CC magma. In Fig. 7, these samples are plotted along the two-component mixing line close to MIX2. As a consequence, we propose that the phase 3 eruption was fed by magma with very similar chemical and isotopic compositions to the CC-type magma (Fig. 8c). Continuation of homogeneous compositions for 4 months after 15 October confirms that the mixing process in phase 2 ended and eruption occurred stably in the central conduits system. Eruptions fed by magmas residing in the central conduits at Mt. Etna had not generally been preceded by significant deformation and volcano-tectonic earthquakes (Patanè et al. 2004, 2005). During phase 3 too, no significant changes in geophysical signals occurred, strengthening the idea that a CC-type magma was, at that time, feeding the activity. It is notable that the effusive eruptive style was unmodified by progressive eruption of CC magma occurring in phases 2 and 3. We might then argue that the new magma rising in the central conduits had already released most of volatile components during continuous degassing in the open conduits of the summit craters (Caltabiano et al. 2004). As a consequence, the

abundance of volatile components was insufficient to make the eruptive style more explosive.

Conclusions

Three phases with different magmatic processes for the 2004-2005 eruption at Mt. Etna can account for chemical variations in major and trace elements and the Sr and Nd isotopic ratios. Petrological data suggest that an isolated batch of the "eccentric" magma had evolved through fractional crystallization after the 2002–2003 eruption. On 7 September 2004, magma in this batch was erupted owing to tectonic stresses controlling the dynamics of the east flank of the volcano. From 24 September until 15 October, the "eccentric" magma batch was progressively mixed with a new magma arriving from the central conduits. Then, the latter magma had been erupted until the end of the eruption.

Mixing of magmas has already been invoked to explain intra-eruptive compositional variations for products of the 1991–1993 (Armienti et al. 1994) and 2001 eruptions at Etna (Viccaro et al. 2006). Furthermore, it is a frequent process in basaltic volcanoes in different geodynamic settings, such as Hawaii, where eruptions occur mainly along rift zones (Garcia et al. 2000; Thornber et al. 2003), and Cerro Azul in Galapagos Islands, where consecutive eruptions have occurred in a sector of the volcano without rift zones (Teasdale et al. 2005). In the above examples, the mixing process mainly involves magma previously stored in a reservoir which is injected by a new mafic magma rising from depth. The study of 2004–2005 eruption at Mt. Etna gives the opportunity to prove that this petrogenetic process may also occur because two different magmas mix owing to tectonic accidents induced by the flank instability of the volcano edifice. Petrologic data of the 2004–2005 lavas proved an important tool for investigating magmatic processes occurring in the shallow plumbing system of Mt. Etna. They contributed to a better understanding of the relationship between petrogenetic processes, eruptive behavior, and instability of the eastern flank of the volcano during an eruptive event. In this context, the 2004–2005 activity teaches us that an eruptive event may be triggered by tectonic accidents and that this process may itself promote the reactivation of the shallow plumbing system, without modifying the effusive eruptive style.

References

Allard P, Behncke B, D'Amico S, Neri M, Gambino S (2006) Mount Etna 1993–2005: anatomy of an evolving eruptive cycle. Earth Sci Rev 78:85–114

Andronico D, Branca S, Calvari S, Burton M, Caltabiano T, Corsaro RA, Del Carlo P, Garfì G, Lodato L, Miraglia L, Murè F, Neri M, Pecora E, Pompilio M, Salerno G, Spampinato L (2005) A multi-disciplinary study of the 2002-03 Etna eruption: insights into a complex plumbing system. Bull Volcanol 67:314–330. doi:10.1007/s00445-004-0372-8

Armienti P, Innocenti F, Petrini R, Pompilio M, Villari L (1988) Sub-aphyric alkali basalt from Mt.Etna: inferences on the depth and composition of the source magma. Rend Soc It Miner Petrol 43:877–891

Armienti P, Clocchiatti R, D'Orazio M, Innocenti F, Petrini R, Pompilio M, Tonarini S, Villari L (1994) The long-standing 1991–1993 Mount Etna eruption. Petrography and Geochemistry of lavas. Acta Vulcanol 4:15–28

Bonaccorso A, Bonforte A, Guglielmino F, Palano M, Puglisi G (2006) Composite ground deformation pattern forerunning the 2004–2005 Mount Etna eruption. J Geoph Res 111:B12207. doi:10.1029/2005JB004206

Burton M, Neri M, Andronico D, Branca S, Caltabiano T, Calvari S, Corsaro RA, Del Carlo P, Lanzafame G, Lodato L, Miraglia L, Salerno G, Spampinato L (2005) Etna 2004–2005: An archetype for geodynamically-controlled effusive eruptions. Geophys Res Lett 32:L09303. doi:10.1029/2005GL022527

Caltabiano R, Burton M, Giammanco S, Allard P, Bruno N, Murè F, Romano R (2004) Volcani gas emissions from the summit craters and flanks of Mt. Etna, 1987-2000. In: Bonaccorso A et al (ed) Mt. Etna: Volcano Laboratory, Geophys. Monogr. AGU, Washington D. C., pp 111–128

Carignan J, Hild P, Mevelle G, Morel J, Yeghicheyan D (2001) Routine analyses of trace elements in geological samples using flow injection and low pressure on-line liquid chromatography coupled to ICP-MS: A study of geochemical reference materials BR, DR-N, UB-N, AN-G and GH. Geostandards Newsletter 25(2, 3):187–198

Clocchiatti R, Condomines M, Guenot N, Tanguy JC (2004) Magma changes at Mount Etna: the 2001 and 2002-2003 eruptions. Earth Planet Sci Lett 226(3, 4):397–414

Corsaro RA, Pompilio M (2004) Magma dynamics at mount etna. In: Bonaccorso et al (ed) Mt. Etna: Volcano Laboratory, Geophys. Monogr. AGU, Washington D. C., pp 91–110

Corsaro RA, Miraglia L (2005) Dynamics of 2004–2005 Mt. Etna effusive eruption as inferred from petrologic monitoring. Geophys Res Lett 32:L13302. doi:10.1029/2005GL022347

Corsaro RA, Miraglia L, Pompilio M (2007) Petrologic evidence of a complex plumbing system feeding the July–August 2001 eruption of Mt. Etna, Sicily, Italy. Bull Volcanol 69:401–421. doi:10.1007/s00445-006-0083-4

Di Grazia G, Falsaperla S, Langer H (2006) Volcanic tremor location during the 2004 Mount Etna lava effusion. Geophys Re Lett 33: L04304. doi:10.1029/2005GL025177

Di Renzo V, Di Vito MA, Arienzo I, Carandente A, Civetta L, D'Antonio M, Giordano F, Orsi G, Tonarini S (2007) Magmatic history of somma-vesuvius on the basis of new geochemical and isotopic data from a deep borehole (Camaldoli della Torre). J Petrol 48(4):753–784

D'Orazio M, Armienti P, Cerretini S (1998) Phenocryst/matrix trace-element partition coefficients for hawaiite-trachyte lavas from the Ellittico volcanic sequence (Mt. Etna, Sicily, Italy). Mineral Petrol 64:65–88. doi:10.1007/BF01226564

Garcia MO, Pietruszka AJ, Rhodes JM, Swanson K (2000) Magmatic processes during the prolonged Pu'u 'O'o eruption of Kilauea volcano, Hawaii. J Petrol 41(7):967–990

Le Maitre RW (Ed.) (2002) Igneous rocks. A classification and glossary of terms. Recommendations of the IUGS Subcomission on the Systematics of Igneous Rocks, 2nd edn. Cambridge University Press, Cambridge, 236 pp

Langmuir CH, Vocke Jr RD, Hanson GN, Hart SR (1978) A general mixing equation with applications to Icelandic basalts. Earth Planet Sci Lett 37(3):380–392. doi:10.1016/0012-821X(78)90053-5

Métrich N, Rutherford MJ (1998) Low pressure crystallization paths of H_2O-saturated basaltic–hawaiitic melts from Mt. Etna: implications for open-system degassing volcanoes. Geochim Cosmochim Acta 62:1195–1205. doi:10.1016/S0016-7037898)00048-9

Metrich N, Allard P, Spilliaert N, Andronico D, Burton M (2004) 2001 flank eruption of the alkali- and volatile-rich primitive basalt responsible for Mount Etna's evolution in the last three decades. Earth Planet Sci Lett 228(1, 2):1–17

Miraglia L (2006) Valutazione dell'accuratezza e della precisione delle analisi eseguite con il sistema analitico SEM-EDS su standard internazionali di minerali e vetri, report UFVG2006/115 http://www.ct.ingv.it/Report/RPTVGPTR20061231.pdf

Neri M, Acocella V (2006) The 2004-05 Etna eruption: Implications for flank deformation and structural behaviour of the volcano. J Volcanol Geotherm Res 158:195–206. doi:0.1016/j.jvolgeores.2006.04.022

Patanè D, Cocina O, Falsaperla S, Privitera E, Spampinato S (2004) Mt. Etna volcano: A seismological framework. In: Bonaccorso A et al (ed) Mt. Etna: Volcano Laboratory, Geophys. Monogr. AGU, Washington D. C., pp 147–165

Patanè D, Mattia M, Aloisi M (2005) Shallow intrusive processes during 2002–2004 and current volcanic activity on Mt. Etna. Geophys Res Lett 32:L06302. doi:10.1029/2004GL021773

Rittmann A (1965) Notizie sull'Etna. Supplemento al Nuovo Cimento 3(I):1117–1123

Spilliaert N, Allard P, Métrich N, Sobolev AV (2006) Melt inclusion record of the conditions of ascent, degassing, and extrusion of volatile-rich alkali basalt during the powerful 2002 flank eruption of Mount Etna (Italy). J Geoph Res 111:B04203. doi:10.1029/2005JB003934

Tanguy JC (1980) L'Etna: Etude pétrologique et paléomagnétique. Implications volcanologiques, PhD Thesis, 520 pp. Universitè Pierre et Marie Curie (Paris 6), Paris, 15 December

Teasdale R, Geist D, Kurz M, Harpp K (2005) 1998 Eruption at Volcán Cerro Azul, Galápagos Islands: I. Syn-Eruptive Petrogenesis. Bull Volcanol 67:170–185

Thornber CR, Heliker C, Sherrod DR, Kauahikaua JP, Miklius A, Okubo PG, Trusdell FA, Budahn JR, Ridley WI, Meeker GP (2003) Kilauea Rift zone magmatism: an episode 54 perspective. J Petrol 44(9):1525–1559. doi:10.1093/petrology/egg048

Viccaro M, Ferlito C, Cortesogno L, Cristofolini R, Gaggero L (2006) Magma mixing during the 2001 event at Mount Etna (Italy): effects on the eruptive dynamics. J Volcanol Geotherm Res 149:139–159